Large-N phase transition in lattice two-dimensional principal chiral models

Massimo Campostrini, Paolo Rossi, and Ettore Vicari
Dipartimento di Fisica dell'Università and INFN, I-56126 Pisa, Italy
(Received 8 February 1995)

We investigate the large-N critical behavior of two-dimensional lattice chiral models by Monte Carlo simulations of U(N) and SU(N) groups at large N. Numerical results confirm strong-coupling analyses, i.e., the existence of a large-N second-order phase transition at a finite β_c.

PACS number(s): 11.15.Me, 11.10.Kk, 11.15.Ha, 11.15.Pg

I. INTRODUCTION

Strong-coupling studies of lattice two-dimensional principal chiral models, with the standard nearest-neighbor interaction

$$S_L = -2N\beta \sum_{x,\mu} \mathrm{Re}\mathrm{Tr}\left[U(x)\, U^\dagger(x+\mu)\right], \qquad \beta = \frac{1}{NT}, \tag{1}$$

have shown evidence of a large-N phase transition at a finite β_c, separating the strong-coupling and the weak-coupling regions [1,2]. An analysis of the 18th-order $N = \infty$ strong-coupling series of the specific heat showed a second-order critical behavior

$$C \sim |\beta - \beta_c|^{-\alpha}, \tag{2}$$

with the following estimates of β_c and α: $\beta_c = 0.3058(3)$ and $\alpha = 0.23(3)$ [2,3]. This critical phenomenon is somehow effectively decoupled from the continuum limit ($\beta \to \infty$); indeed, dimensionless ratios of physical quantities are reproduced with great accuracy even for $\beta < \beta_c$ [4,2].

Large-N critical behaviors are also present in single-matrix systems and are in general related to the continuum limit of two-dimensional gravity models. In particular the Gross-Witten single-link model shows at $N = \infty$ a third-order phase transition at $\beta_c = 1/2$ with a specific-heat critical exponent $\alpha = -1$ [5]. We recall that the partition function of one-dimensional lattice chiral models [and also of two-dimensional QCD (QCD_2) with a Wilson action] can be reduced to that of the Gross-Witten single-link model, thus leading to the same critical properties.

In this paper we investigate the large-N critical phenomenon of two-dimensional lattice principal chiral models by Monte Carlo simulations, that is, by extrapolating, possibly in a controlled manner, numerical results at sufficiently large N, in the same spirit of the double-scaling limit technique developed in the studies of one-dimensional matrix models. We performed Monte Carlo simulations of SU(N) and U(N) models for several large values of N, studying the approach to $N = \infty$. Some SU(N) Monte Carlo results at large N were already presented in Ref. [4]. Since SU(N) and U(N) models are expected to have the same large-N limit, U(N) Monte Carlo results provide further information and a check of the $N \to \infty$ behavior of lattice principal chiral models.

In the continuum limit SU(N) and U(N) two-dimensional lattice actions should describe the same theory even at finite N, in that the additional U(1) degrees of freedom of the U(N) models decouple. The U(N) lattice action, when restricting ourselves to its SU(N) degrees of freedom, represents a different regularization of the SU(N)$\times$SU(N) chiral field theory. One-loop calculations in perturbation theory give the Λ-parameter ratios

$$\frac{\Lambda_{\overline{\mathrm{MS}}}}{\Lambda_L^{\mathrm{U}}} = \sqrt{32}\, \exp\left(\frac{\pi}{2}\right), \tag{3}$$

$$\frac{\Lambda_L^{\mathrm{SU}}}{\Lambda_L^{\mathrm{U}}} = \exp\left(\frac{\pi}{N^2}\right), \tag{4}$$

where Λ_L^{U} and Λ_L^{SU} are, respectively, the Λ parameters of the U(N) and SU(N) lattice actions (1) and $\overline{\mathrm{MS}}$ denotes the modified minimal subtraction scheme.

The fundamental group-invariant correlation function of SU(N) models is

$$G(x) = \frac{1}{N}\left\langle \mathrm{Tr}\left[U^\dagger(x) U(0)\right]\right\rangle. \tag{5}$$

Introducing its lattice momentum transform $\widetilde{G}(p)$, we define the magnetic susceptibility $\chi = \widetilde{G}(0)$, and the second-moment correlation length

$$\xi_G^2 = \frac{1}{4\sin^2\pi/L}\left[\frac{\widetilde{G}(0,0)}{\widetilde{G}(0,1)} - 1\right]. \tag{6}$$

In the U(N) case we consider two Green's functions. One describes the propagation of SU(N) degrees of freedom:

$$G(x) = \frac{1}{N}\left\langle \mathrm{Tr}[\hat{U}^\dagger(x)\hat{U}(0)]\right\rangle, \qquad \hat{U}(x) \equiv \frac{U(x)}{[\det U(x)]^{1/N}}. \tag{7}$$

The other describes the propagation of the U(1) degrees of freedom associated with the determinant of $U(x)$:

$$G_d(x) = \left\langle \left\{\det[U^\dagger(x) U(0)]\right\}^{1/N}\right\rangle. \tag{8}$$

From the Green's functions $G(x)$ and $G_d(x)$ we can define the corresponding magnetic susceptibilities χ, χ_d and second-moment correlation lengths ξ_G, ξ_d.

At finite N, while SU(N) lattice models do not have any singularity at finite β, U(N) lattice models should undergo a phase transition, driven by the U(1) degrees of freedom corresponding to the determinant of $U(x)$, and following a pattern similar to the two-dimensional XY model [6]. The mass propagating in the determinant channel M_d should vanish at a finite value β_d and stay zero for larger β. Then for $\beta > \beta_d$ this sector of the theory decouples from the other [SU(N)] degrees of freedom, which are those determining the continuum limit of principal chiral models for $\beta \to \infty$. We recall that the two-dimensional XY model critical behavior is characterized by a sharp approach to the critical point β_{XY} (the correlation length grows exponentially), a line of fixed point for $\beta > \beta_{XY}$, and a finite specific heat having a peak for a $\beta < \beta_{XY}$ (see, e.g., Ref. [7]).

II. NUMERICAL RESULTS

A. Monte Carlo algorithm

In our simulations we used local algorithms containing overrelaxation precedures. In the SU(N) case, we employed the Cabibbo-Marinari algorithm [8] to upgrade SU(N) matrices by updating their SU(2) subgroups, chosen randomly among the $\frac{N(N-1)}{2}$ subgroups acting on each 2×2 submatrix. At each site the SU(2) subgroup identified by the indices i, j ($1 \leq i < j \leq N$) was updated with a probability $P = \frac{2}{N-1}p$, so that the average number of SU(2) updatings per SU(N) site variable was $\bar{n} = pN$. In our simulations we always chose $p \lesssim 1$, decreasing p when increasing N. We used $p \simeq 1$ at $N = 9$, $p \simeq 2/3$ at $N = 15$ and $p \simeq 1/2$ at $N = 21, 30$. The extension to the U(N) case is easily achieved by updating, beside SU(2) subgroups, U(1) subgroups. In our simulations we upgraded the U(1) subgroups identified by the diagonal elements of the U(N) matrix. The SU(2) and U(1) updatings were performed by a mixture of an overheat-bath algorithm [9] (90%) and a standard heat-bath algorithm (10%). At a fixed parameter p, the number of operations per site increases as N^2 at large N.

The above algorithm experiences a critical slowing down in N; that is, keeping the correlation length fixed the autocorrelation time grows with increasing N. This effect is partially compensated by a reduction of the fluctuations of group-invariant quantities when N grows. In the U(N) simulations the quantities related to the determinant channel are subjected to large fluctuations, causing large errors in the measurements.

In Tables I and II we present Monte Carlo data, respectively, for the U(N) and SU(N) simulations. Finite-size systematic errors in evaluating infinite-volume quantities should be smaller than the statistical errors of all numerical results presented in this paper.

TABLE I. Numerical results for U(N).

N	β	L	Stat	E	C	χ	ξ_G	χ_d	ξ_d
9	0.30	24	100k	0.60374(8)	0.284(6)	10.50(3)	2.058(14)	1.64(2)	0.6(2)
	0.31	30	150k	0.56706(9)	0.427(11)	15.43(4)	2.649(17)	2.82(4)	1.0(2)
	0.313	30	300k	0.55215(10)	0.541(11)	18.53(5)	2.972(14)	3.93(5)	1.2(2)
	0.315	36	150k	0.54077(14)	0.61(2)	21.80(10)	3.36(3)	5.59(9)	1.9(2)
	0.318	36	300k	0.52128(10)	0.66(2)	29.47(9)	4.08(3)	11.3(2)	3.0(2)
	0.3185	36	400k	0.51799(11)	0.69(2)	31.17(11)	4.22(2)	12.8(2)	3.2(2)
	0.319	42	300k	0.51482(11)	0.69(2)	32.86(13)	4.38(3)	14.7(4)	3.3(3)
	0.320	42	400k	0.50816(10)	0.66(2)	37.2(2)	4.73(3)	20.5(5)	4.3(3)
	0.323	48	330k	0.49172(9)	0.50(2)	51.6(3)	5.83(4)	55(3)	8.5(5)
	0.323	60	200k	0.49166(11)	0.52(2)	51.7(3)	5.79(7)	57(3)	7.7(7)
15	0.28	18	150k	0.65373(4)	0.163(3)	6.924(7)	1.519(4)	1.030(8)	
	0.30	24	200k	0.60276(6)	0.300(10)	10.81(2)	2.063(9)	1.29(2)	
	0.305	24	180k	0.58405(9)	0.396(12)	13.09(3)	2.346(9)	1.57(2)	
	0.308	30	250k	0.56875(9)	0.57(2)	15.55(3)	2.632(10)	2.14(2)	0.7(2)
	0.310	30	300k	0.55423(12)	0.78(3)	18.83(5)	2.996(11)	3.31(5)	1.2(2)
	0.311	30	500k	0.54453(10)	0.97(4)	21.58(4)	3.276(8)	4.87(6)	1.6(1)
	0.311	36	300k	0.54470(13)	0.97(4)	21.52(6)	3.276(14)	4.85(9)	1.5(2)
	0.312	36	600k	0.53374(11)	1.05(4)	25.57(10)	3.67(2)	8.42(15)	2.8(2)
	0.313	36	500k	0.52365(12)	0.94(4)	30.42(10)	4.131(15)	14.5(5)	3.7(3)
	0.315	42	200k	0.50920(10)	0.50(3)	40.0(2)	4.95(4)	42(5)	7.2(7)
	0.315	48	300k	0.50915(7)	0.49(2)	39.7(2)	4.89(4)	46(3)	8.1(7)
21	0.28	18	100k	0.65373(4)	0.162(4)	6.972(8)	1.526(5)	0.991(8)	
	0.30	24	200k	0.60273(6)	0.303(9)	10.881(13)	2.069(6)	1.140(8)	
	0.3025	24	300k	0.59390(6)	0.361(10)	11.869(14)	2.185(6)	1.220(9)	
	0.305	30	300k	0.58318(6)	0.446(14)	13.31(2)	2.364(9)	1.394(11)	
	0.308	30	200k	0.56337(15)	0.88(6)	16.79(5)	2.748(13)	2.15(3)	
	0.309	30	300k	0.5512(3)	1.31(13)	19.92(10)	3.09(2)	3.60(9)	1.2(2)
	0.3095	30	450k	0.5415(3)	1.98(15)	23.11(13)	3.43(2)	6.6(3)	2.4(2)
	0.31	36	300k	0.5337(2)	1.28(10)	26.23(11)	3.75(2)	11.1(5)	3.4(3)

TABLE II. Numerical results for SU(N). When more than one lattice size appears, the corresponding results were obtained collecting data of simulations at the reported lattice sizes (which were, in all cases, in agreement within the errors).

N	β	L	Stat	E	C	χ	ξ_G
9	0.290	30	200k	0.58774(8)	0.412(7)	13.32(3)	2.353(11)
	0.294	30,36	600k	0.56788(6)	0.435(6)	16.89(3)	2.793(14)
	0.295	24,30,36,42	900k	0.56284(4)	0.443(5)	18.00(2)	2.910(9)
	0.2955	36	500k	0.56026(5)	0.442(6)	18.58(4)	2.95(2)
	0.296	30,36	600k	0.55781(5)	0.438(6)	19.20(3)	3.03(2)
	0.2965	36	600k	0.55531(6)	0.436(6)	19.86(4)	3.08(2)
	0.300	30,36,42	350k	0.53846(9)	0.413(11)	25.27(7)	3.66(2)
	0.310	42,48,54	500k	0.50030(4)	0.306(5)	47.25(12)	5.43(3)
15	0.295	24	200k	0.60013(11)	0.47(2)	11.47(2)	2.149(9)
	0.299	30	300k	0.57564(10)	0.66(2)	15.07(3)	2.577(11)
	0.300	24	400k	0.56798(10)	0.69(4)	16.55(3)	2.738(6)
	0.300	30	400k	0.56805(10)	0.70(3)	16.57(3)	2.746(9)
	0.300	36	600k	0.56807(9)	0.66(2)	16.58(2)	2.745(8)
	0.300	42	500k	0.56810(5)	0.70(2)	16.57(3)	2.752(12)
	0.3005	36	600k	0.56430(7)	0.68(2)	17.41(3)	2.833(11)
	0.301	36	500k	0.56054(6)	0.68(2)	18.31(3)	2.940(10)
	0.302	36	500k	0.55300(5)	0.65(2)	20.26(3)	3.131(9)
	0.305	36	500k	0.53418(6)	0.516(13)	26.86(6)	3.786(11)
	0.310	45	300k	0.51178(4)	0.354(7)	39.06(10)	4.80(2)
21	0.300	24	300k	0.58810(10)	0.65(3)	12.90(2)	2.310(6)
	0.302	30	500k	0.57049(13)	1.00(4)	15.91(3)	2.665(7)
	0.302	36	600k	0.57069(8)	0.95(3)	15.87(2)	2.659(8)
	0.3025	24	400k	0.56490(20)	1.14(6)	17.09(6)	2.787(8)
	0.3025	30	400k	0.56517(14)	1.02(5)	17.02(4)	2.784(8)
	0.3025	36	500k	0.56491(11)	1.04(5)	17.11(4)	2.800(10)
	0.303	36	500k	0.55959(9)	0.96(4)	18.38(3)	2.936(9)
	0.305	30	500k	0.54100(8)	0.72(2)	24.14(5)	3.526(8)
	0.310	42	240k	0.51548(6)	0.41(2)	36.66(12)	4.61(2)
30	0.300	24	150k	0.59927(8)	0.38(2)	11.35(2)	2.114(7)
	0.3025	30	200k	0.58479(10)	0.79(5)	13.24(3)	2.338(7)
	0.303	30	200k	0.58007(15)	1.00(8)	13.99(4)	2.433(10)
	0.304	24	500k	0.5625(4)	2.4(3)	17.55(7)	2.857(10)
	0.304	30	500k	0.5632(3)	2.3(2)	17.40(7)	2.829(8)
	0.305	30	200k	0.5466(2)	1.05(10)	22.13(5)	3.320(12)

B. Numerical evidence of a large-N phase transition

Lattice chiral models have a peak in the specific heat

$$C = \frac{1}{N}\frac{dE}{dT}, \tag{9}$$

which becomes sharper and sharper with increasing N. In Figs. 1 and 2 we plot the specific heat, respectively, for the U(N) and SU(N) models. Such a behavior of the specific heat should be an indication of a phase transition for $N = \infty$ at a finite β_c. The positions of the peaks $\beta_{\rm peak}$ in SU(N) and U(N) converge from opposite directions, restricting the possible values of β_c to $0.304 \lesssim \beta_c \lesssim 0.309$. Notice that Monte Carlo data for $\beta \lesssim \beta_c \simeq 0.306$ approach, for growing N, the resummed 18th-order large-N strong-coupling series of the specific heat [3]; in this region, as expected by strong-coupling considerations, the convergence of U(N) models is faster.

A more accurate estimate of the critical coupling β_c can be obtained by using a finite-N scaling ansatz

$$\beta_{\rm peak}(N) \simeq \beta_c + cN^{-\epsilon}, \tag{10}$$

in order to extrapolate $\beta_{\rm peak}(N)$ to $N \to \infty$. The above ansatz is suggested by the idea that the parameter N may play a role quite analogous to the volume in ordinary systems close to the criticality. This idea was already exploited in the study of one-dimensional matrix models [10–12], where the double-scaling limit turned out to be very similar to finite-size scaling in a two-dimensional critical phenomenon. Substituting $L \to N$ and $1/\nu \to \epsilon$, Eq. (10) becomes the well-known finite-size scaling relationship derived in the context of renormalization group theory. Furthermore, the exponent ϵ should be the same in the U(N) and SU(N) models, in that it should be a critical exponent associated with the $N = \infty$ phase transition. Notice that the function $\beta_{\rm peak}(N)$ in Eq. (10) is considered at infinite space volume.

In the study of ordinary critical phenomena the reweighting technique [13], turns out to be very efficient to determine quantities such as the position of the specific-heat peak. In our work we could use this technique only for $N = 9$, since for larger N the reweighting range around the point where the simulation is performed

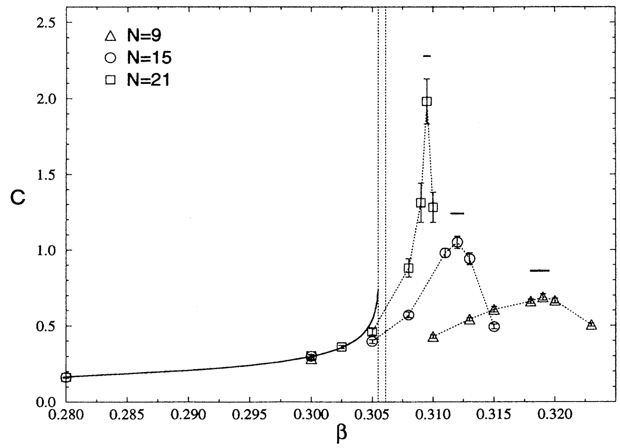

FIG. 1. Specific heat vs β for SU(N) models. The solid line represents the strong-coupling determination, whose estimate of the critical β is indicated by the vertical dashed lines. The thick solid lines above the peaks represent our estimates of β_{peak}.

turned out to be much smaller than the typical β interval of our simulations. For $N \geq 15$, $\beta_{\text{peak}}(N)$ data and their errors were estimated from the specific-heat data reported in Tables I and II, supported by the direct measurements of the specific-heat derivatives at each β.

Our estimates of β_{peak} at $N = 9, 15, 21$ for U(N) and $N = 9, 15, 21, 30$ for SU(N) fit very well formula (10). By a fit with four free parameters β_c, ϵ, $c_{\text{U}(N)}$, and $c_{\text{SU}(N)}$, we found

$$\begin{aligned} &\beta_c = 0.3057(3), \\ &\epsilon = 1.45(8). \end{aligned} \tag{11}$$

In Fig. 3 the fit result is compared with the $\beta_{\text{peak}}(N)$ data. A fit with two independent ϵ exponents $\epsilon_{\text{U}(N)}$ and $\epsilon_{\text{SU}(N)}$ gave compatible results, but larger errors. Notice that this Monte Carlo estimate of β_c is in agreement

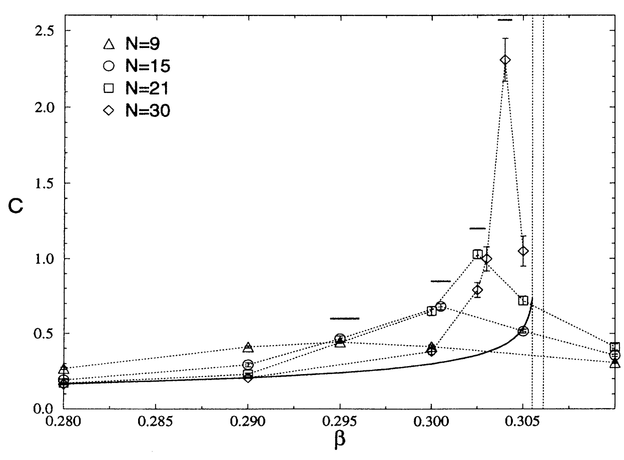

FIG. 2. Specific heat vs β for U(N) models. The solid line represents the strong-coupling determination, whose estimate of the critical β is indicated by the vertical dashed lines. The large solid lines above the peaks represent our estimates of β_{peak}.

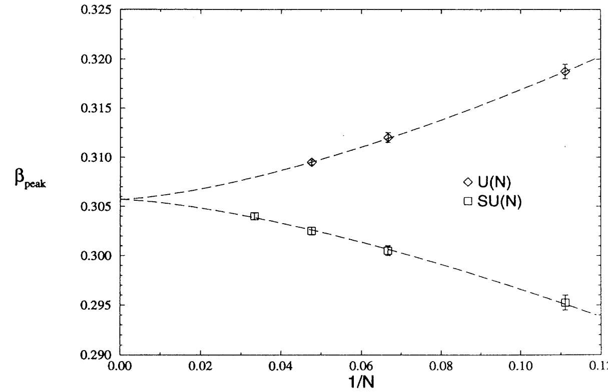

FIG. 3. $\beta_{\text{peak}}(N)$ vs $1/N$. The dashed lines show the fit result.

with the determination (2) coming from strong-coupling computations.

We checked the finite-N scaling ansatz (10) in the similar context of the large-N Gross-Witten phase transition of one-dimensional lattice U(N) chiral models with free boundary conditions, where the critical point β_c and the critical exponents ν and α are known: $\beta_c = 1/2$, $\nu = 3/2$, and $\alpha = -1$. We computed the position of the specific-heat peak at finite N finding the asymptotic behavior (10) with $\epsilon = 2/3$. Details of these calculations are given in the Appendix. Therefore we have $\epsilon = 1/\nu$, as expected from the analogy with the finite-size scaling phenomenon of an ordinary critical system. Notice that the critical exponents ν and α satisfy a two-dimensional hyperscaling relation $2\nu = 2 - \alpha$. In one-dimensional lattice chiral models the number $d_e = 2$ of effective dimensions of the large-N critical phenomenon is related to the fact that the double limit $N \to \infty$ and $\beta \to \beta_c$ is equivalent to the continuum limit of a two-dimensional gravity model with central charge $c = -2$.

Since the large-N phase transition of the two-dimensional lattice chiral models is of the second-order type, its behavior cannot be found in the classification of double-scaling limits of Refs. [14, 15], which are parametrized by a central charge $c < 1$ implying $\alpha < 0$. Moreover, unlike one-dimensional lattice chiral models, the interpretation of the large-N phase transition of two-dimensional lattice chiral models as an effective $d_e = 2$ ordinary critical phenomenon does not seem to be valid: In fact, if $\epsilon = 1/\nu$, by substituting our estimates of α and ϵ in the hyperscaling relation $d_e = (2-\alpha)\epsilon$ we would obtain $d_e = 2.6(2)$. A more general thermodynamic inequality would give $d_e \geq (2-\alpha)\epsilon$ [16].

Monte Carlo data of χ and ξ_G for $\beta \lesssim \beta_c$ compare very well with the large-N strong-coupling series of χ (up to 15th order) and ξ_G (up to 14th order) [2]. Figure 4, where ξ_G is plotted versus β, shows that data approach, with growing N, the curve obtained by resumming the strong-coupling series of ξ_G [3], and in particular the U(N) data, whose convergence is faster, are in quantitative agreement.

Large-N numerical results seem to indicate that all physical quantities, such as χ and ξ_G, are well-behaved

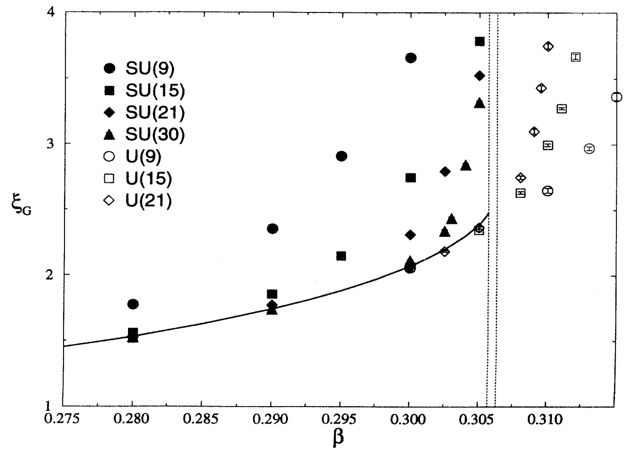

FIG. 4. ξ_G vs β. The solid line represents the strong-coupling determination, whose estimate of the critical β is indicated by the vertical dashed lines.

functions of the internal energy E even at $N = \infty$ [4]. Therefore as a consequence of the specific-heat divergence at β_c, the $N = \infty$ β function $\beta_L(T) \equiv -adT/da$ should have a nonanalytical zero at β_c, that is, $\beta_L(\beta) \sim |\beta-\beta_c|^\alpha$ in the neighborhood of β_c. By defining a new temperature proportional to the energy [17], this singularity disappears, and one can find good agreement between the measured mass scale and the asymptotic scaling predictions in the "energy" scheme even for $\beta < \beta_c$, where strong-coupling expansion is expected to converge [4]. In fact strong-coupling computations show asymptotic scaling with a surprising accuracy of few percent [2].

In the U(N) case, a Kosterlitz-Thouless phase transition driven by the determinant is expected at $\beta_d > \beta_{\rm peak}$ for each finite N. Our data seem to support this picture; indeed, after the peak of C, the magnetic susceptibility χ_d and the second-moment correlation length ξ_d defined from the determinant correlation function (8) begin to grow very fast. In Fig. 5 we plot χ_d versus β. Green and

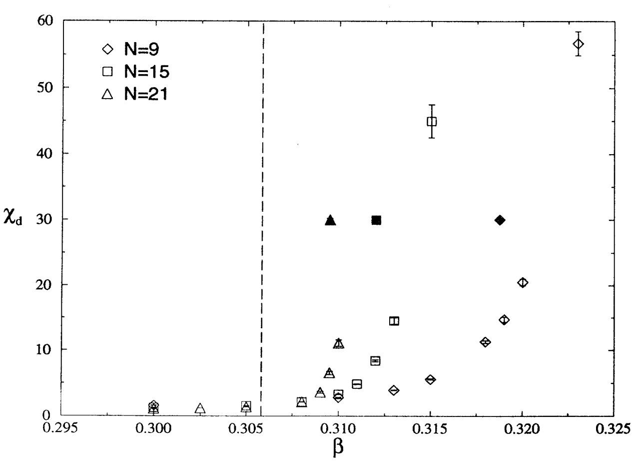

FIG. 5. χ_d vs β. The vertical dashed line indicates the estimate of β_c. The solid symbols indicate the positions of the peak of C at $N = 9, 15, 21$.

Samuel argued (using strong-coupling and weak-coupling arguments) that the large-N phase transition is nothing but the large-N limit of the determinant phase transition present in the U(N) lattice models [6, 18]. According to this conjecture, in the large-N limit β_d and $\beta_{\rm peak}$ should both converge to β_c, and the order of the determinant phase transition would change from an infinite order of the Kosterlitz-Thouless mechanism to a second order with divergent specific heat. The large-N phase transition of the SU(N) models could then be explained by the fact that the large-N limit of the SU(N) theory should be the same as the large-N limit of the U(N) theory. Our numerical results give only a partial confirm of this scenario; we can just get a hint from the behavior of χ_d and ξ_d with growing N that the expected phase transition is moving toward β_c. The large-N strong-coupling series of the mass M_d propagating in the determinant channel has been calculated up to 6th order, indicating a critical point, determined by the zero of the M_d series, slightly larger than our determination of β_c: $\beta_d(N = \infty) \simeq 0.324$ [6]. This discrepancy could be explained either by the shortness of the strong-coupling series of M_d or by the fact that such a determination of β_c relies on the absence of nonanalyticity points before the strong-coupling series of M_d vanishes, and therefore a nonanalyticity at $\beta_c \simeq 0.306$ would invalidate all strong-coupling predictions for $\beta > \beta_c$.

C. Phase distribution of the link operator

In one-dimensional principal chiral models the large-N third-order phase transition is a consequence of a compactification of the eigenvalues of the link operator

$$L = U(x)U^\dagger(x + \mu), \tag{12}$$

which are of the form $\lambda = e^{i\theta}$. In the weak-coupling region ($\beta > \beta_c$) the phase distribution of the eigenvalues of the link operator L, $\rho(\beta, \theta)$ with $\theta \in (-\pi, \pi]$, is nonvanishing only in the region $|\theta| \leq \theta_c(\beta) < \pi$. The third-order critical point β_c is determined by the limit condition $\theta_c(\beta) = \pi$, separating the weak-coupling region from the strong-coupling region where $\rho(\beta, \pi) > 0$ [5].

In order to see if a similar phenomenon characterizes the large-N phase transition also in two dimensions, we have extracted from our simulations the phase distribution $\rho(\beta, \theta)$ of the eigenvalues of L. Notice that $\rho(\beta, \theta) = \rho(\beta, -\theta)$ by symmetry; therefore, in the following we will show $\rho(\beta, \theta)$ only in the range $0 \leq \theta \leq \pi$. Large-N numerical results seems to support the compactification of the phase distribution at β_c; indeed, we found $\rho(\beta, \pi) \simeq 0$ for $\beta \gtrsim \beta_{\rm peak}$ [$\rho(\beta, \pi)$ can be strictly zero only for $N = \infty$]. This fact is illustrated in Fig. 6, where we compare the distributions $\rho(\beta, \theta)$ at $\beta = 0.300$ and $\beta = 0.305$ for $N = 21$, whose $\beta_{\rm peak} \simeq 0.3025$: The distribution values at $\theta = \pi$ ($\rho(0.300, \pi) \simeq 0.010$ and $\rho(0.305, \pi) \simeq 0.0007$) decrease by about a factor of 15, becoming very small. Similar behaviors are observed at the other values of N.

In the SU(N) models $\rho(\beta, \theta)$ presents N maxima, as Fig. 6 shows. This structure is absent in the U(N) models

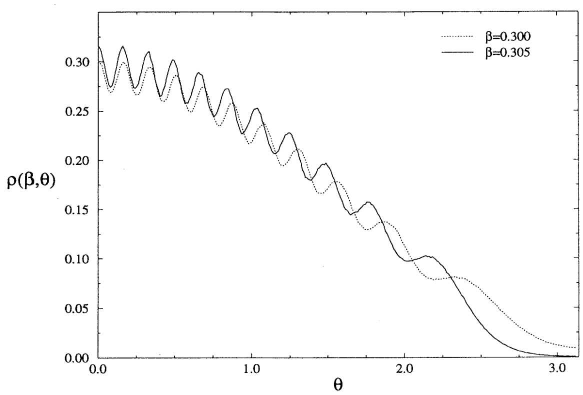

FIG. 6. $\rho(\beta,\theta)$ for the SU(21) model at $\beta = 0.300$ and $\beta = 0.305$.

and should disappear in the large-N limit, in that the height of the peaks with respect to the background curve should vanish. For example, the U(N) and SU(N) phase distributions at $\beta = 0$ are, respectively,

$$\rho(0,\theta) = \frac{1}{2\pi} \tag{13}$$

and

$$\rho(0,\theta) = \frac{1}{2\pi}\left[1 + (-1)^{N+1}\frac{2}{N}\cos(N\theta)\right]. \tag{14}$$

In our SU(N) simulations we found the peak heights to decrease approximately as $1/N$.

It is also interesting to see how the distributions $\rho(n,\beta,\theta)$ of the generalized link operators

$$L(n) = U(x)U^\dagger(x+n\mu) \tag{15}$$

$[\rho(1,\beta,\theta) \equiv \rho(\beta,\theta)]$ evolve as function of the distance n. In Fig. 7 we plot $\rho(n,\beta,\theta)$ for $N = 15$, at $\beta = 0.305$ ($\xi_G \simeq 3.79$), and for various values of n. When $d \equiv n/\xi \to \infty$, $\rho(n,\beta,\theta)$ appears to tend to the $\beta = 0$ distribution (14).

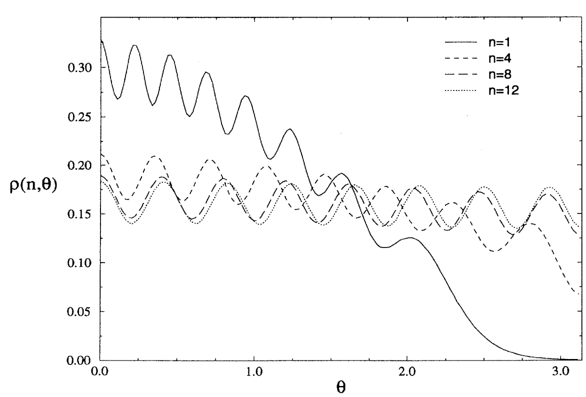

FIG. 7. $\rho(n,\beta,\theta)$ for the SU(15) model at $\beta = 0.305$ for various value of n.

D. Critical slowing down around the large-N singularity

The large-N critical behavior causes a phenomenon of critical slowing down in the Monte Carlo simulations. At sufficiently large N ($N \gtrsim 15$) and for both U(N) and SU(N) models, the autocorrelation times of the internal energy τ_E and the magnetical susceptibility τ_χ (estimated by a blocking procedure) showed a maximum around the peak of the specific heat, and a sharper and sharper behavior with growing N. The increase of the autocorrelation times, with growing N, was much larger around the specific-heat peak than elsewhere. In the SU(N) simulations, τ_E (τ_χ) went from ~ 600 (400) at $\beta = 0.3025$ and $N = 21$ to ~ 3000 (2500) at $\beta = 0.304$ and $N = 30$ (the uncertainty in these numbers is large; they are just indicative). After the peak of C, τ_E and τ_χ decreased, for example, at $N = 30$ and $\beta = 0.305$, $\tau_E \simeq 700$ and $\tau_\chi \simeq 300$. A similar behavior was observed in the U(N) simulations. The above critical slowing-down phenomenon represents the most serious difficulty in getting numerical results around β_c at larger N by the Monte Carlo algorithm used in this work. At large correlation length τ_χ increases again due the critical slowing down associated with the continuum limit, while τ_E tends to be stable.

We want to mention an attempt for a better algorithm in the U(N) case, by constructing a microcanonical updating involving globally the U(N) matrix instead of using its subgroups. A microcanonical updating of U according to the action

$$A(U) = \mathrm{Re}\,\mathrm{Tr}\,[UF] \tag{16}$$

can be achieved by performing the reflection with respect to the U(N) matrix $U_{\max}$ which maximizes $A(U)$:

$$U_{\rm new} = U_{\max}\, U^\dagger_{\rm old}\, U_{\max},$$
$$U_{\max} = \frac{1}{\sqrt{F^\dagger F}}F^\dagger. \tag{17}$$

Notice that the determination of $U_{\max}$ requires the diagonalization of the complex matrix F. The update (17) does not change the action, and it must be combined with ergodic algorithms (e.g., heat bath). We found that, at large N and in the region of β values we considered, the algorithm based on the SU(2) and U(1) subgroups performs better than those based on the updating (17). The latter may become convenient at relatively small N and/or for larger correlation lengths. On the other hand, at large space correlation lengths multigrid algorithms should eventually become more efficient, in that they should have smaller dynamical exponents (see Refs. [19, 20] for some implementations of multigrid algorithms in the context of lattice chiral models).

APPENDIX

The partition function of the one-dimensional U(N) chiral model can be reduced to that of a single unitary matrix model, i.e., the Gross-Witten model

TABLE III. $\beta_{\mathrm{peak}}(N)$ and $C(N, \beta_{\mathrm{peak}})$ versus N for one-dimensional U(N) lattice chiral models.

N	β_{peak}	$C(\beta_{\mathrm{peak}})$
2	0.930889	0.29461215
3	0.818356	0.27992604
4	0.758001	0.27269388
5	0.719664	0.26839003
6	0.692846	0.26553250
7	0.672876	0.26349442
8	0.657337	0.26196545
9	0.644848	0.26077452
10	0.634554	0.25981956
11	0.625899	0.25903594

$$Z(N, \beta) = \int dU \exp(N\beta \operatorname{Tr}[U + U^\dagger]). \tag{A1}$$

The free energy density can then be written in terms of a determinant of modified Bessel functions

$$F(N, \beta) = \frac{1}{N^2} \ln Z(N, \beta) = \frac{1}{N^2} \ln \det I_{j-i}(2N\beta). \tag{A2}$$

The large-N limit of the specific heat,

$$C(N, \beta) = \frac{1}{N} \frac{dE}{dT} = \frac{1}{2} \beta^2 \frac{d^2 F}{d\beta^2}, \tag{A3}$$

shows the existence of a third-order phase transition at $\beta_c = 1/2$; indeed, we have

$$C(\infty, \beta) = \beta^2 \quad \text{for} \quad \beta \leq \beta_c,$$
$$C(\infty, \beta) = \frac{1}{4} \quad \text{for} \quad \beta \geq \beta_c. \tag{A4}$$

The singularity at β_c can be characterized by a negative critical exponent $\alpha = -1$. It is worth noting that an analysis of the double scaling $N \to \infty$ and $\beta \to \beta_c$ allows the determination of the correlation length exponent $\nu = 3/2$ [21], and that α and ν satisfy a hyperscaling relationship associated with a two-dimensional critical phenomenon: $2\nu = 2 - \alpha$.

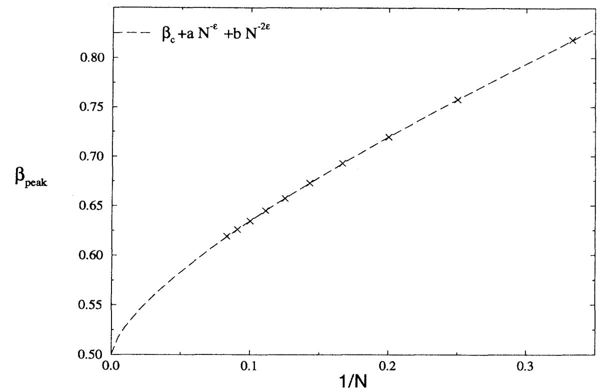

FIG. 8. $\beta_{\mathrm{peak}}(N)$ vs $1/N$ in one-dimensional U(N) lattice chiral models.

One-dimensional U(N) lattice chiral models present a peak in the specific heat, whose position $\beta_{\mathrm{peak}}(N)$ should approach β_c with increasing N. The finite-N scaling arguments already mentioned in this paper lead to the ansatz (10) for the positions of the specific heat peaks. In Table III we report the values of $\beta_{\mathrm{peak}}(N)$ and $C(N, \beta_{\mathrm{peak}})$ as function of N up to $N = 11$. As shown in Fig. 8, the large-N behavior of $\beta_{\mathrm{peak}}(N)$ is well fitted by

$$\beta_{\mathrm{peak}}(N) = \beta_c + aN^{-\epsilon} + bN^{-2\epsilon}, \tag{A5}$$

with $\epsilon = 2/3$, and therefore $\nu = 1/\epsilon = 3/2$ ($a \simeq 0.595$ and $b \simeq 0.13$). The result $\nu = 3/2$ was also found in the finite-N scaling of the partition function zeros [12].

[1] F. Green and S. Samuel, Nucl. Phys. **B190**, 113 (1981).
[2] M. Campostrini, P. Rossi, and E. Vicari, Phys. Rev. D **51**, 958 (1995).
[3] M. Campostrini, P. Rossi, and E. Vicari, Phys. Rev. D **52**, 358 (1995), paper I; preceding paper, **52**, 386 (1995).
[4] P. Rossi and E. Vicari, Phys. Rev. D **49**, 6072 (1994); **50**, 4718(E) (1994).
[5] D. J. Gross and E. Witten, Phys. Rev. D **21**, 446 (1980).
[6] F. Green and S. Samuel, Phys. Lett. **103B**, 110 (1981).
[7] R. Gupta and C. Baillie, Phys. Rev. D **45**, 2883 (1992).
[8] N. Cabibbo and E. Marinari, Phys. Lett. **119B**, 387 (1982).
[9] R. Petronzio and E. Vicari, Phys. Lett. B **254**, 444 (1991).
[10] J. W. Carlson, Nucl. Phys. **B248**, 536 (1984).
[11] E. Brezin and J. Zinn-Justin, Phys. Lett. B **288**, 54 (1992).
[12] P. H. Damgaard and U. M. Heller, Nucl. Phys. **B410**, 494 (1993).
[13] A. M. Ferrenberg and R. H. Swendsen, Phys. Rev. Lett. **61**, 2635 (1988); **63**, 1196 (1989).
[14] E. Brezin and V. Kazakov, Phys. Lett. B **236**, 144 (1990).
[15] D. Gross and A. Migdal, Phys. Rev. Lett. **64**, 127 (1990).
[16] H. E. Stanley, *Introduction to Phase Transitions and Critical Phenomena* (Clarendom Press, Oxford, 1971).
[17] G. Parisi, in *High Energy Physics 1980*, Proceedings of the XXth Conference on High Energy Physics, Madison, Wisconsin, 1980, edited by L. Durand and L. G. Pondrom, AIP Conf. Proc. No. 68 (AIP, New York, 1981).
[18] F. Green and S. Samuel, Nucl. Phys. **B194**, 107 (1982).
[19] R. G. Edwards, S. J. Ferreira, J. Goodman, and A. D. Sokal, Nucl. Phys. **B380**, 621 (1992).
[20] M. Hasenbusch and S. Meyer, Phys. Rev. Lett. **68**, 435 (1992).
[21] V. Periwal and D. Shevitz, Phys. Rev. Lett. **64**, 1326 (1990).